Thermodynamic and Experimental Study on the Modification of Nonmetallic Inclusions Through the Contact with $CaO-Al_2O_3-MgO$ Slags

Susanne K. Michelic, Mario Hartl, Christian Bernhard,
Chair of Metallurgy, Montanuniversitaet Leoben
Franz-Josef-Straße 18, Leoben, 8700, Austria
Phone-(0043) 3842 402 2214
Fax-(0043) 3842 402 2202
E-mail: susanne.michelic@unileoben.ac.at

Key words: Inclusions, Slags, Thermodynamics, Modification, SEM/EDS analysis, Tammann furnace, Laser Scanning Confocal Microscope

INTRODUCTION

Due to the wide field of application of steels, the demands on their properties advance continuously. One of the major factors significantly influencing the final product quality is the cleanness of steels. Whether the mechanical properties or the behavior under corrosive media is concerned, non-metallic inclusions (NMI) often are decisive for material defects. Besides the number and distribution of NMIs, mainly their size, shape and composition are essential. In order to achieve the cleanness requirements, a continuous optimization of the liquid steelmaking process is necessary. Over the last years, the broad topic "Steel Cleanness" has become one of the main research points at the Chair of Metallurgy. Next to the improvement of characterization methods, the primary target is to combine thermodynamic modeling and laboratory experiments in order to describe the changes in inclusion landscape under different conditions.

The steel cleanness can particularly be influenced in the processes of secondary metallurgy. Thus, the understanding of reactions and interactions between steel, slag, refractory material and NMIs is a fundamental aspect regarding process optimization. Inclusion removal can take place in different aggregates (e.g. in the ladle or in the tundish) by transportation of the inclusions to the steel/slag interface, separation at the steel/slag interface and subsequent dissolution in the slag. Basically, oxide-slag systems consisting of the components $CaO-Al_2O_3-MgO-SiO_2$ are common in secondary metallurgical processes. Several researchers dealt with the modification of inclusions due to steel-slag interactions in the last years [1-3]. Different laboratory setups in combination with subsequent metallographic analyses were used to particularly study the behavior of $MgO-Al_2O_3$ spinels, because this inclusion type often causes defects due to its high melting point and high hardness. A very effective method for an in-situ observation of the dissolution of oxides in different slag compositions is the Laser Scanning Confocal Microscope (LSCM), which offers the possibility to determine the effect of slag composition on the dissolution time of inclusions [4-7]. In the present work, the modification behavior of oxides through the contact with the slag system $CaO-Al_2O_3-MgO$ is examined out of a thermodynamic as well as an experimental viewpoint. For the thermodynamic calculations the commercial software FactSage 6.1 is used. Experiments on laboratory scale are carried out in a Tammann Furnace followed by detailed manual and automated SEM/EDS analyses. The effect of slag composition on the resulting number, shape and composition of the non-metallic inclusions is discussed, also considering aspects of agglomeration and separation. In addition, first results of experiments with the LSCM are shown, giving essential information on the dissolution behavior of oxides in $CaO-Al_2O_3$ slags.

THERMODYNAMIC MODELING

The thermodynamic calculations assuming equilibrium conditions were done with the "Equilib" tool of FactSage 6.1 using the databases FToxid and FSstel. Based on calculations of the single components steel, slag and NMI, a thermodynamic description of the system steel-slag-inclusion for the defined conditions was established. In the present work, a low-alloyed, Ca-treated carbon steel was used for the calculations as well as in the experimental part; its composition is shown in Table I. Table II summarizes the three different slag compositions which were applied.

Table I. Steel composition used for thermodynamic modeling and laboratory experiments.

wt.-% C	wt.-% Mn	wt.-% Si	wt.-% Al	wt.-% O	wt.-% S
0.16	0.57	0.83	0.021	0.011	0.0045

Table II. Slag compositions used for thermodynamic modeling and laboratory experiments.

	wt.-% CaO	wt.-% Al_2O_3	wt.-% MgO
Slag 1	50	50	-
Slag 2	20	65	15
Slag 3	33	34	33

The "Phase Diagram" module of FactSage 6.1 was used to determine the liquid surface projection of the system CaO-Al_2O_3-MgO as a function of temperature. In Figure 1 two different states are shown for each slag variation:

1. Basic composition of the three slags at room temperature (see also Table I)
2. Composition of the three slags at 1600 °C.

It can be seen that in contrast to slag 1, which is part of the binary system CaO-Al_2O_3, slag 2 is saturated with $MgO{\cdot}Al_2O_3$ and slag 3 is saturated with MgO. Furthermore, it must be mentioned that the influence of the crucible was only calculated for the case without slag addition. In the calculations with the three different slags, the crucible was not considered. More details on the calculation procedure as well as detailed results can be found in a previous work[8].

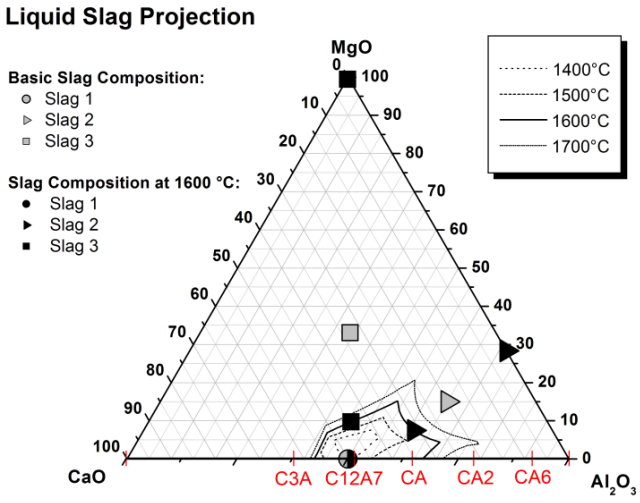

Figure 1. Projection of the liquid slag phase of the system CaO-Al_2O_3-MgO as a function of temperature.

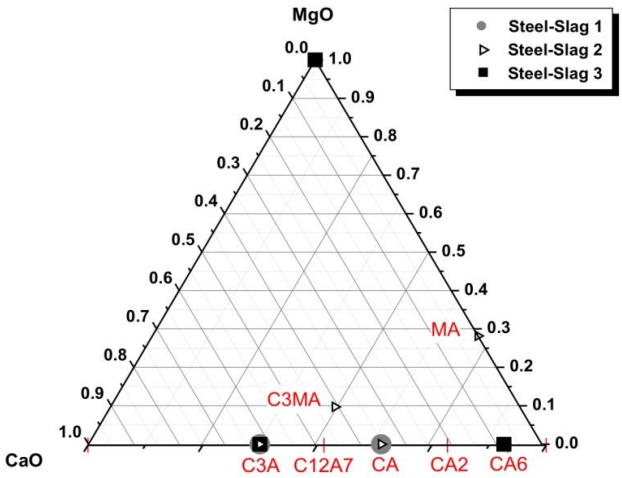

Figure 2. Stable phases of NMI according to thermodynamic calculations for the steel in combination with different slag compositions.

EXPERIMENTAL PRODECUDURE

Experiments on Laboratory Scale

A low-alloyed, Ca-treated carbon steel was melted in a 20 kg induction furnace (see Table I). The melt was fully deoxidized with Al, a CaFe-wire was used for Ca-treatment, no slag was added during melting. These experimental conditions were chosen consciously, resulting in a relatively high oxygen content compared to industrial processes and therefore a high number of NMI. Samples out of this basic alloy were remelted in a Tammann furnace with additions of different slags followed by SEM/EDS analyses for inclusions characterization. The detailed test sequence is shown in Figure 3. The Tammann furnace is a high-temperature electric resistance furnace, which can be heated up to 2000 °C. Due to the carbon heating tubes inside the furnace and their reaction with the residual oxygen, the final oxygen content in the furnace vessel is extremely low (0.001 ppm). The schematic experimental setup for the remelting experiments as well as the furnace itself is shown in Figure 4. All experiments in the Tammann furnace were carried out under Ar-atmosphere (Argon 5.0), using a sample weight of 300 g steel. The samples were heated up to 1600 °C; this temperature was held for 10 min. In order to study the influence of the used crucible on the final inclusion landscape, in a first step two experiments were carried out without slag addition and varying crucible material. In order to study the influence of the refractory material, both an Al_2O_3 and a MgO crucible were used. In the second phase, the described slags were added to the crucible covering the whole steel bath surface (the slag mass equals appr. 5 % of the steel mass). For every slag, three experiments were performed under the same conditions. For all experiments with slag addition an Al_2O_3 crucible was used.

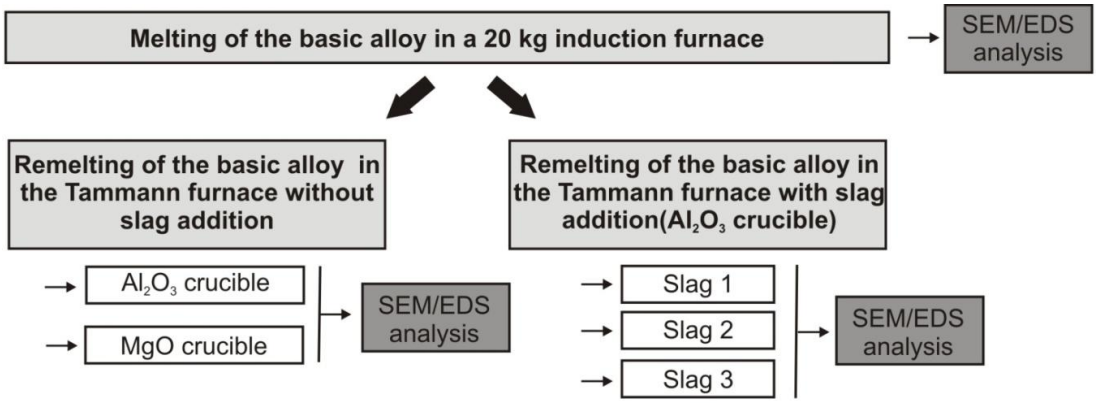

Figure 3. Illustration of the test sequence.

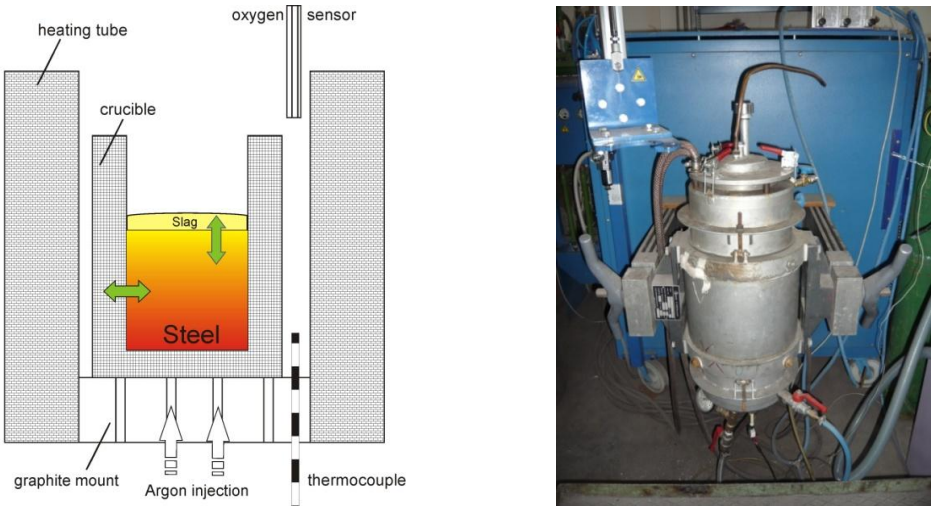

a) b)

Figure 4. a) Schematic illustration of the test arrangement and b) photograph of the Tammann furnace used for laboratory experiments.

Metallographic Analyses

After the experiments the steel samples were prepared metallographically and analyzed by manual and automated SEM/EDS analyses. Figure 5a shows a schematic cross section of the crucible with the remelted sample. In order to also study possible agglomeration effects at the top of the sample, for automated SEM/EDS analyses the measuring area was defined on the vertical section, as illustrated in Figure 5b, covering the total sample height.

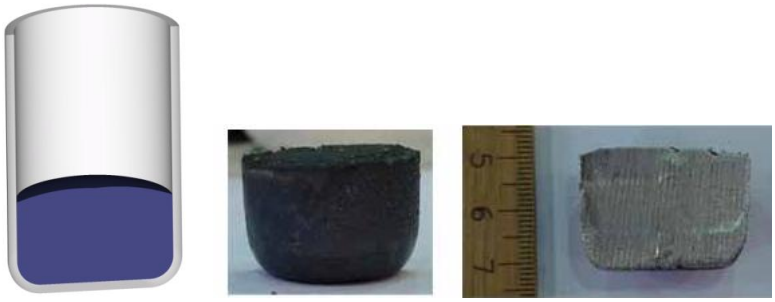

a) b)

Figure 5. a) Schematic section through the crucible and the sample b) photograph of a remelted sample and the vertical section of the sample.

In automated SEM/EDS analysis, non-metallic inclusions are detected due to material contrast differences in the backscattered electron (BSE) image. The output of automated SEM/EDS analyses regarding the properties of non-metallic inclusions consists of morphological data of every detected particle as well as its chemical composition and the corresponding EDS spectrum. In addition, in order to get an impression of the sample homogeneity, the distribution of the non-metallic inclusions over the whole sample area is registered. Thus, the possibility of rapidly relocating any particle can be assured, which is a very useful tool in order to manually verify untypical particles after the automated measurement. In general, all inclusion types can be detected simultaneously during the measurement. For the present investigation, a Scanning Electron Microscope manufactured by Fei (Quanta 200 MK2) is used in combination with an EDS system of Oxford Instruments (INCA).

Laser Scanning Confocal Microscope

In order to study the dissolution behavior of inclusions in the slags used in the Tammann furnace, experiments were carried out in the LSCM. The experimental setup at the Chair of Metallurgy consists of a LSCM attached to a high temperature furnace. The LSCM is equipped with extra-long distance objectives. In order to be out of the characteristic spectrum of samples with temperatures up to 1600 °C, the wavelength of the laser is 405 nm. The gold coated chamber of the infrared furnace has the shape of a symmetric ellipse where the halogen lamp is in the bottom focal point; the crucible is in the upper focal point. It is possible to use oxidizing or reducing

atmosphere and vacuum down to 10^{-8} bar, the highest temperature is 1700 °C (short time) with a maximum heating rate of 1000 °C per minute. Cooling rates are dependent to the temperature between 1000 °C per minute down to 800 °C without quenching. The used experimental setup as well as the time-temperature profile of the present experiments is shown in Figure 6. Al_2O_3 particles with a grain size of 100 mesh were added to the cold pre-fused cylinder of CaO-Al_2O_3 slag (slag 1 in Table 2). The sample was rapidly heated to 1200 °C under Ar Atmosphere with heating rate of 400 °C/min. Heating rate to 1390 °C was 100 °C/min, after that the temperature was controlled manually up to 1465 °C, where the particles were completely dissolved after a holding time of about 100 s. For reason of homogenization the temperature was held for another 2 min before cooling.

a) b)

Figure 6. a) Schematic illustration of sample and crucible configuration in the LSCM b) Time-temperature profile used in the experiments.

RESULTS AND DISCUSSION

In the following, the results of automated SEM/EDS analyses for the different experiments are described and compared to the thermodynamic calculations. In addition, some details of manual analyses are presented for a better understanding of the occurring modification reactions. Finally, the results of the LSCM experiments are shown. A typical inclusion in the initial state of the steel before remelting in the Tammann furnace is exemplarily shown in Figure 7. The results of the automated SEM/EDS analyses are displayed in Figure 8 and 9. The position of the detected oxides in the ternary system CaO-Al_2O_3-MgO is shown in each case. For the ternary systems only oxide inclusions (tolerating 2 wt.-% S at most) are considered in the evaluations. For all comparisons with slag experiments, for the case without slag addition the results of remelting in the Al_2O_3 crucible are used.

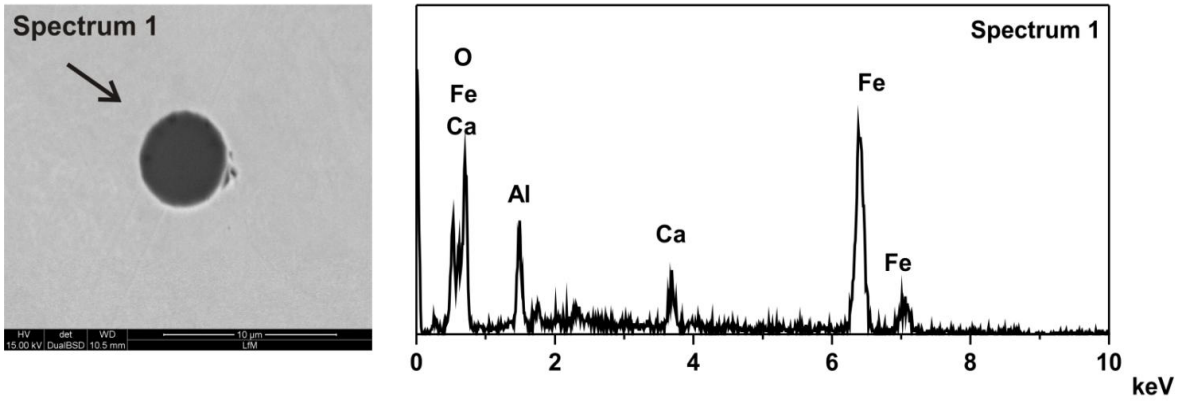

a) b)

Figure 7. a) SEM-image of a CaO-Al_2O_3 inclusion in the initial state before remelting b) Corresponding EDS spectrum.

Influence of the Crucible Material on the Inclusion Composition

The initial state of the inclusion landscape, meaning the state before remelting is shown in Figure 8a. Evidently, nearly all oxides are part of the two phase system CaO-Al_2O_3, mainly located at the Al_2O_3-rich side. As displayed in Figure 8b, the remelting of the basic material in the Al_2O_3 crucible leads to a remarkable displacement of the inclusion towards the Al_2O_3 corner. Using a MgO crucible, a noticeable movement of the inclusions to the two phase system MgO-Al_2O_3 system is found. These results show that the significant influence of the refractory material, which always has to be considered when interpreting experimental results.

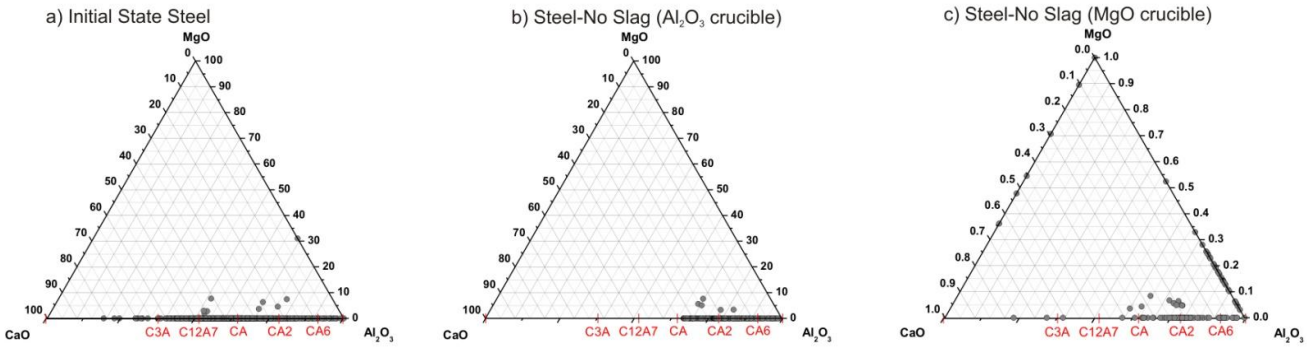

Figure 8. Experimental results of the automated SEM/EDS analyses of a) the initial state in the basic material and b) the remelted alloy without slag addition (Al_2O_3 crucible) and c) the remelted alloy without slag addition (MgO crucible).

Modification of Inclusions through Different Slag Compositions

Regarding the results of the experiments with further slag addition (Figure 9), very interesting changes can be observed. While slag 1 does not change the initial state significantly (apart from a slight drift to higher Al_2O_3 contents, which can partly be attributed to the influence of the crucible), slags 2 and 3 have a higher impact on the resulting inclusion landscape. Slag 3 substantially changes the composition of the inclusions towards higher MgO contents.

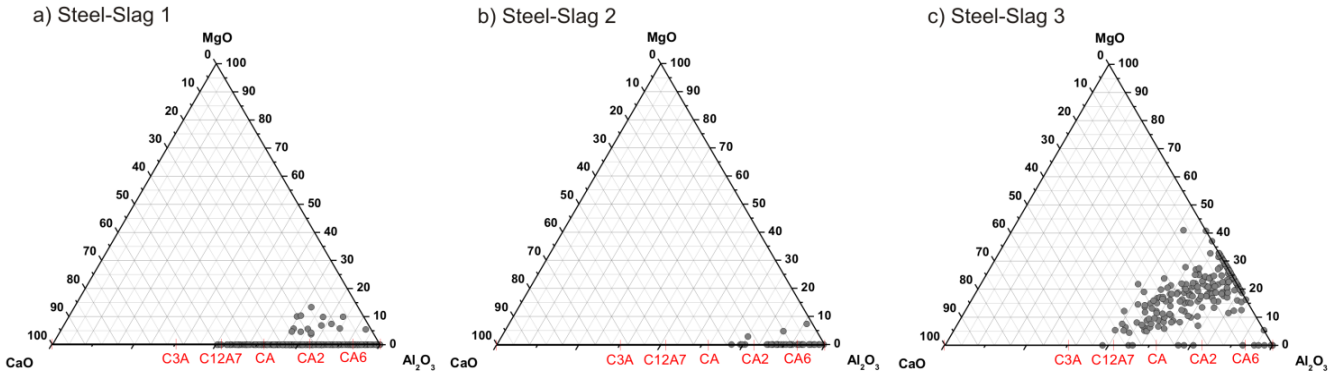

Figure 9. Experimental results of the automated SEM/EDS analyses for the remelted alloy with slag addition: a) slag 1, b) slag 2 and c) slag 3.

Figure 10 shows the modification ratio CaO/Al_2O_3 of the different experimental cases in terms of a scatter band of mean±standard deviation. The figure summarizes the observations made above: Starting from a relatively broad scatter band in the initial state, remelting with slag 1 does not significantly modify the inclusion landscape (apart from the influence of the crucible). Conversely, remelting with slags 2 and 3 creates inclusions with more Al_2O_3 content; with slag 2 having the greatest influence. Figure 11 and Figure 12 exemplify SEM-mappings of typical inclusions detected in the samples remelted with slag 2 and slag 3. As illustrated in Figure 11, the inclusion landscape not only shows a strong movement towards the Al_2O_3 corner through remelting with slag 2, but also the bordering of the oxide with a slight sulfide layer. An example for an inclusion with MgO core surrounded by a $CaO-Al_2O_3$ as a result of remelting the steel with slag 3 is given in Figure 12.

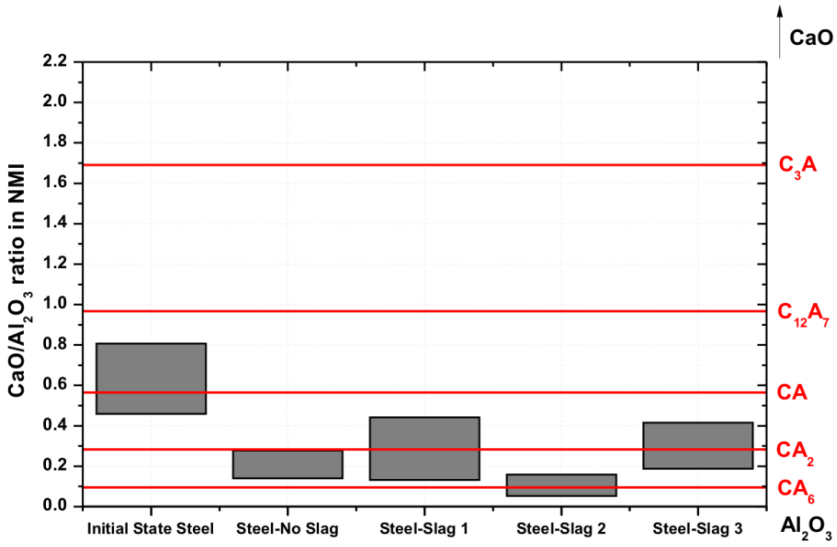

Figure 10. Comparison of modification ratio between the different experimental cases.

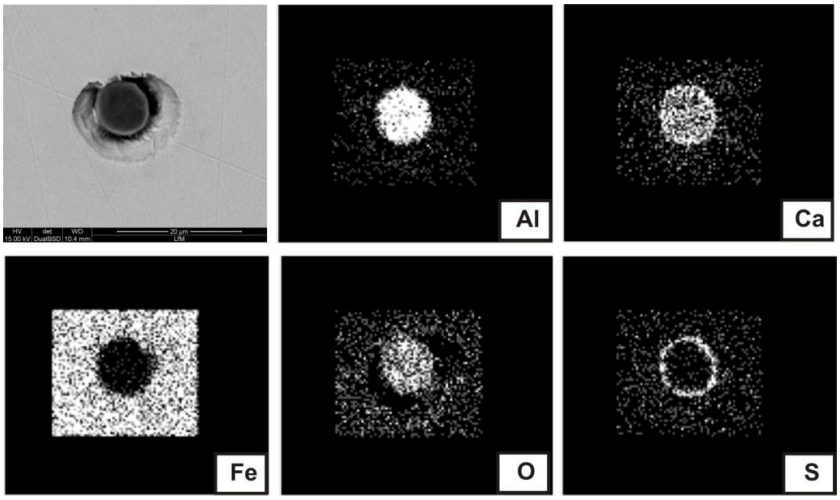

Figure 11. SEM-mapping of a CaO-Al_2O_3 inclusion surrounded by a sulfide seam after remelting with slag 2.

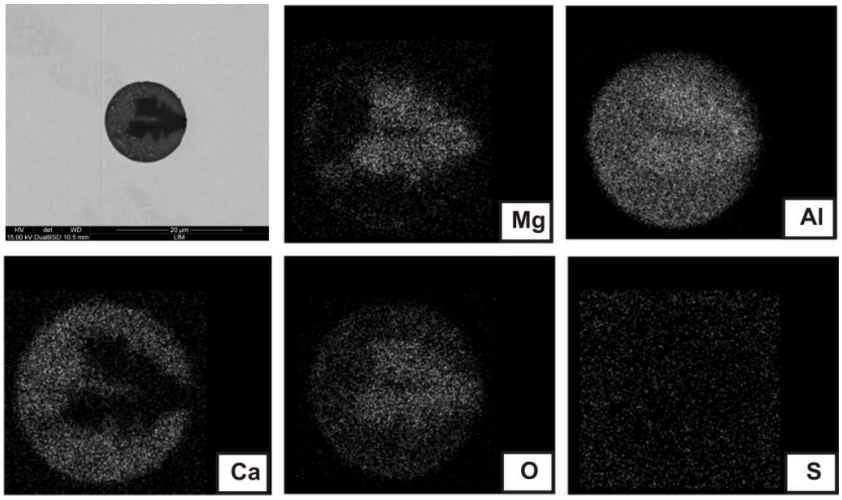

Figure 12. SEM-mapping of a complex CaO-Al_2O_3-MgO inclusion after remelting with slag 3.

Changes in Number of Inclusions and Inclusion Content

Next to the modification of inclusions through the addition of different slags, also a significant decrease of the overall number of NMI as well as the overall inclusion content per mm^2 can be observed. In comparison to the initial state, slag 1 seems to be the most efficient slag for inclusion absorption (see Figure 13). For all experiments with slag addition a good agreement of decrease in number and inclusion content can be observed. In contrast, although a decrease in number is measured for the experiment without slag addition, Figure 13b shows that in the present case the overall inclusion content increases through remelting without slag addition. In this experimental case it can be observed that, next to a possible growth of the particles, the inclusions had no possibility of separating at the steel/slag interface. Moreover, they had enough time in the steel melt for reacting with the crucible material. However, the decrease in number can be explained by the agglomeration of particles at the top of the steel sample: Comparing the SEM-images in the initial state and in the remelted case without slag addition in Figure 14 a remarkable agglomeration is observed.

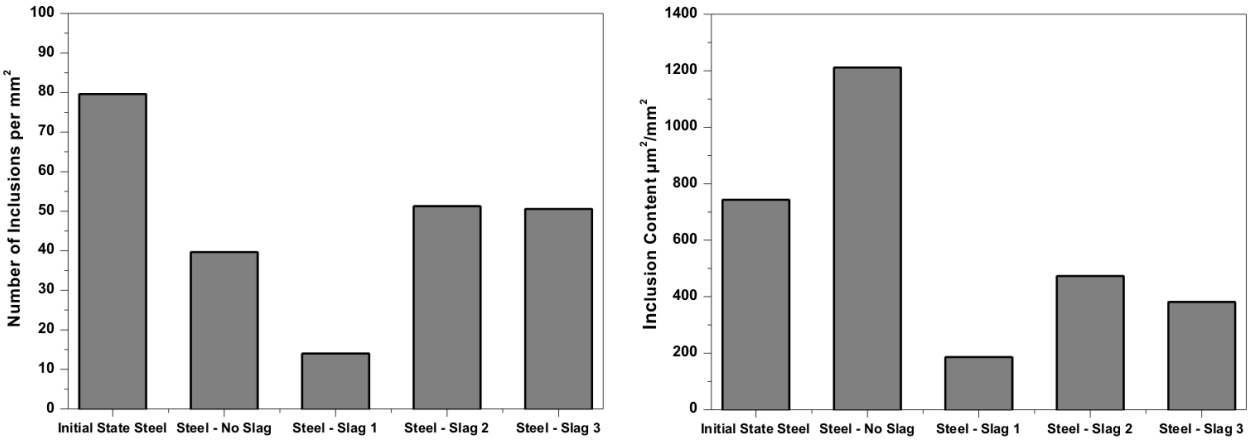

a) b)

Figure 13. a) Changes in number of inclusions per mm^2 for the different experimental cases;
b) Changes in inclusion content for the different experimental cases.

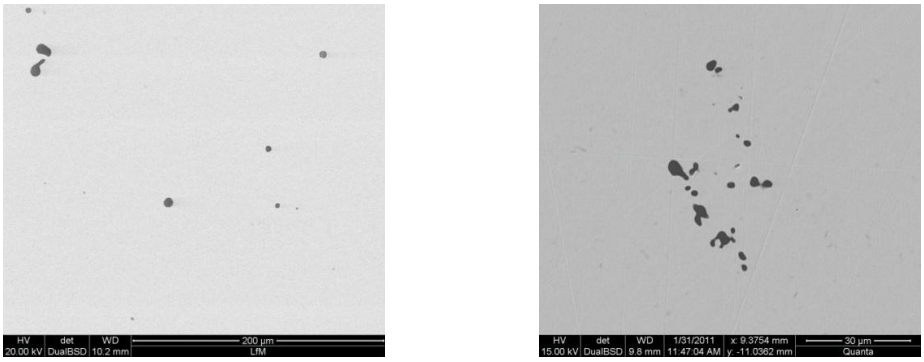

a) b)

Figure 14. a) Distribution of inclusions in the initial state of the melted steel;
b) Distribution of inclusions after remelting without slag addition at the top of the sample.

Comparison between Laboratory Experiments and Calculations

Although the possible reaction time in the experiments is comparatively long, only conditions near the equilibrium are obtained. Furthermore, as already shown in the results, the separation of NMI, and other kinetic aspects – which are not considered in the calculations – influence the resulting inclusion landscape.

Due to the high content of Al_2O_3 in slag 2, the inclusions remarkably move towards the Al_2O_3 corner and are finally situated between CA2 and CA6. In contrast to the calculated results, no $MgO{\cdot}Al_2O_3$ are detected in the metallographic analyses. In this case the calculated solid $MgO{\cdot}Al_2O_3$ are part of the slag phase. This can well be explained by the fact that solid particles in the slag covering the steel, will hardly interact with the steel owing to the higher density of the steel. In the sample remelted with slag 3 a significant

MgO content in inclusions was measured with SEM/EDS analyses. In this case a possible explanation may be the reaction of the solved MgO in the slag with the crucible and/or with the steel respectively the NMI. Pertaining to Figure 1, it can be seen that the content of solved MgO in the slag at 1600 °C is higher for slag 3 than for slag 2 (9.7 vs. 7.5 % solved MgO, respectively). Obviously this slight difference already influences the formation of $MgO{\cdot}Al_2O_3$ according to the above stated mechanism. In addition, comparing the activities of the slag components at 1600 °C (see Table III), it is obvious that in case of slag 2 the $a(Al_2O_3)$ is by far the highest, whereas $a(MgO)\approx 1$ in slag 3, which also gives an indication for the resulting inclusion landscape. Although the thermodynamic calculations are a good indication for the modification of the inclusion landscape, further investigations are required to explain the discrepancy between the calculated results and the experimental analyses.

Table III. Activities of the slag components calculated with FactSage 6.1;
Reference states are pure solid Al_2O_3, pure solid MgO and pure solid CaO.

	a(CaO)	**$a(Al_2O_3)$**	**a(MgO)**
Slag 1	0.137	0.218	0.000
Slag 2	0.020	0.880	0.058
Slag 3	0.204	0.069	0.995

Dissolution Behavior of Al_2O_3 in CaO-Al_2O_3 Slag

As already shown in the results of automated SEM/EDS analyses, slag 1 seems to offer the best absorption behavior for non-metallic inclusions. For this reason, slag 1 was chosen for the experiments with the LSCM. Figure 15 illustrates the behavior of the distributed Al_2O_3 particles at different time steps and temperatures. At about 1350 °C little pools of molten slag around the Al_2O_3 occurred and the particles started to dissolve. As soon as the slag phase was completely liquid, the particles tend to agglomerate and were continuously dissolved in the slag in less than 100 s. So far, only a qualitative analysis of the dissolution behavior has been done. In a next step, also a quantitative determination of dissolution rates as a function of particle size is intended and further experiments with varying slag compositions are planned.

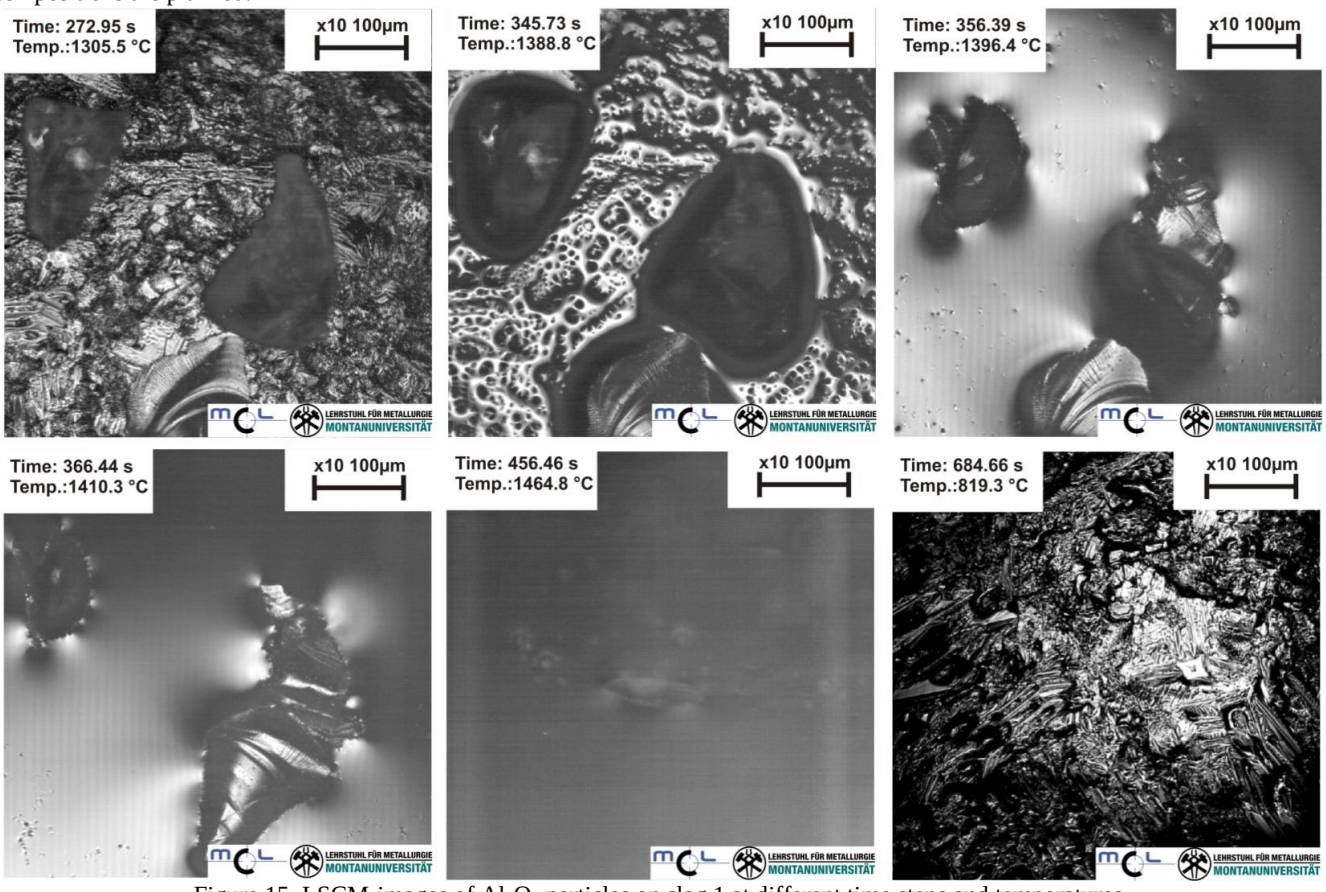

Figure 15. LSCM-images of Al_2O_3 particles on slag 1 at different time steps and temperatures.

SUMMARY AND CONCLUSION

The present work focused on the modification behavior of oxides through the contact with $CaO\text{-}Al_2O_3\text{-}MgO$ slags. Thermodynamic calculations were compared with experiments on laboratory scale and subsequent SEM/EDS analyses. Furthermore, a Laser Scanning Confocal Microscope was used for in-situ observation of the dissolution of particles in a $CaO\text{-}Al_2O_3$ slag. Several combinations showed a high degree of conformity between the predictions made by the thermodynamic software FactSage 6.1; in one case a discrepancy was observed which requires further investigation of the occurring mechanisms. This combination of thermodynamic modeling and experimental simulation offers a powerful tool to study the reactions and interactions between steel, slag and refractory material regarding the formation and modification of non-metallic inclusions. Although several aspects that influence the experiments cannot be simulated theoretically, the calculations yield feasible indications for further process investigations. The properly designed and controlled experiments facilitate the adjustment and assessment of thermodynamic models and also provide fundamental knowledge for the development of kinetic models for isolated phenomena, affecting steel cleanness.

REFERENCES

1. M. Jiang, X.H. Wang and W.J. Wang, „Control of Non-metallic Inclusions by Slag-metal Reactions for High Strength Alloying Steels", *steel research international*, Vol. 81, No.9, 2010, pp.759-765.
2. J.H: Park and D.S. Kim, "Effect of $CaO\text{-}Al_2O_3\text{-}MgO$ Slags on the Formation of MgO Al_2O_3 Inclusions in Ferritic Stainless Steel", *Metallurgical and Materials Transactions B*, Vol.36B, 2005, pp.495-502.
3. M. Jiang, X. Wang, B. Chen and W. Wang, „Formation of MgO Al_2O_3 Inclusions in High Strength Alloyed Structural Steels Refined by $CaO\text{-}SiO_2\text{-}Al_2O_3\text{-}MgO$ Slag", *ISIJ International*, Vol. 48, No. 7, 2008, pp.885-890.
4. B.J. Monaghan and L.Chen, "Effect of changing slag composition on spinel inclusion dissolution", *Ironmaking and Steelmaking*, Vol. 33, No.4, 2006, pp. 323-330.
5. B.J. Monaghan, L.Chen and J. Sorbe, "Comparative study of oxide inclusion dissolution in $CaO\text{-}SiO_2\text{-}Al_2O_3$ slag", *Ironmaking and Steelmaking*, Vol. 32, No.3, 2005, pp.258-264.
6. M. Valdez et al., "Dissolution of Inclusions in Steelmaking Slags", *ISSTech 2003 Conference Proceedings*, pp. 789-798.
7. K.W. Yi et al., "Determination of dissolution time of Al_2O_3 and MgO inclusions in synthetic $Al_2O_3\text{-}CaO\text{-}MgO$ slags", *Scandinavian Journal of Metallurgy*, Vol. 32, 2003, pp. 177-184.
8. S.K. Michelic, M.Hartl and C. Bernhard: "Interactions of non-metallic inclusions with steel and slag: Thermodynamic Modeling, Experiments and Metallographic Analyses", *EPD Congress 2011: Materials Processing Fundamentals*, 2011.